

DR with a DSLR: Digital Radiography with a Digital Single-Lens Reflex camera

Helen Fan^{*a,b}, Heather L. Durko^{a,b}, Stephen K. Moore^{b,c}, Jared Moore^{a,b}, Brian W. Miller^{a,b},
Lars R. Furenlid^{a,b,c}, Sunil Pradhan^d, Harrison H. Barrett^{a,b,c}

^aCollege of Optical Sciences, University of Arizona, Tucson, AZ 85721

^bDept. of Radiology and Center for Gamma Ray Imaging, University of Arizona, Tucson AZ 85724

^cProgram in Biomedical Engineering, University of Arizona, Tucson AZ 85721

^dDepartment of Radiology, Tribhuvan University Teaching Hospital, Kathmandu, Nepal

ABSTRACT

An inexpensive, portable digital radiography (DR) detector system for use in remote regions has been built and evaluated. The system utilizes a large-format digital single-lens reflex (DSLR) camera to capture the image from a standard fluorescent screen. The large sensor area allows relatively small demagnification factors and hence minimizes the light loss. The system has been used for initial phantom tests in urban hospitals and Himalayan clinics in Nepal, and it has been evaluated in the laboratory at the University of Arizona by additional phantom studies. Typical phantom images are presented in this paper, and a simplified discussion of the detective quantum efficiency of the detector is given.

Keywords: Digital radiography, single-lens reflex camera, x-ray screen, detectability, DQE, Nepal.

1. INTRODUCTION

Access to modern digital radiology (DR) is very limited in developing countries [1]. The Himalayan regions of Nepal, India, Pakistan and Tibet present special difficulties because of lack of adequate roads, inconsistent or nonexistent power grids, little internet access and few trained physicians. In Nepal, for example, all of the remote district hospitals and many health outposts have x-ray facilities, but they are all film-based. There are very few resident radiologists, and teleradiology is rare [1,2].

The goal of the work reported in this paper is to develop an inexpensive DR system intended for wide dissemination in the Himalayan regions of Nepal and other rural areas in developing countries. The basic approach is simple: just photograph a fluorescent screen exposed to x rays. This is an old idea that has been proposed and rejected many times. The basic problem is that the optical sensors used in digital cameras are much smaller than, say, a chest x ray. Therefore the camera must be moved far from the fluorescent screen so that the entire x ray image fits on the sensor. That means that most of the light from the screen misses the lens, and the small amount of light that reaches the sensor is lost in the electronic readout noise of the camera.

Several recent technological developments have, however, come together to change this situation completely. The latest generation of digital single-lens reflex cameras (DSLRs), such as the Nikon D700 and the Canon 5D, have much larger sensors than were available even a year or two ago, so the camera can be placed closer to the screen, thereby subtending a larger solid angle and collecting more light. Because these cameras are intended for general consumer use, they are quite inexpensive, in the range of just \$2,000 – \$2,500. In spite of the low cost, however, they have excellent noise performance, even compared to expensive scientific-grade CCD cameras. Moreover, new lenses designed especially for use with DSLRs concentrate the light efficiently onto the active area of the sensor.

*hxfan@email.arizona.edu; phone 1-520-626-6963

In Sec. 2 we discuss the technical issues that must be considered in the design of a DR system based on DSLRs, and in Sec. 3 we analyze the effect of detector noise and inefficient light collection on lesion detectability. In Sec. 4, we describe a compact prototype system that we built and tested both in Nepal and at the University of Arizona. Some of the results of these tests are presented in Sec. 5, and a summary and conclusions are presented in Sec. 6.

2. DESIGN CONSIDERATIONS

2.1. Cameras and lenses

The DSLRs considered here are “full field” cameras, which means that the sensor is approximately the same size as a frame of 35 mm film (24 mm × 36 mm). This format is also referred to in the DSLR world as FX. Cameras in this class include the Canon 5D and 5D Mark II and the Nikon D700, D3X and D3S. Even larger sensors are also available; for example the MegaVision E6 which has a 37 mm × 49 mm sensor, but it is substantially more expensive than the “prosumer” (professional/consumer) full-field cameras.

A 24 mm × 36 mm sensor operated at 12:1 demagnification will allow the imaging of 29 cm × 43 cm field of view (FOV), adequate for chest radiography. For comparison, a 37 mm × 49 mm sensor will cover a comparable field at 8:1 demagnification. Of course, smaller FOVs require proportionally smaller demagnification factors. With a full-field camera, a 12 cm × 18 cm FOV can be achieved at 5:1 demagnification.

Almost all of the cameras under discussion are color cameras. The color selectivity is achieved by placing color filters over the photosensitive pixels, with usually half of the pixels sensitive to green light, a quarter of them sensitive to blue light and a quarter to red light. Black-and-white DSLRs are not currently available (except for the MegaVision E6, which can be shipped without the filters), though there would be considerable interest in them among serious photographers. For purposes of this paper, the color filters are a distinct drawback because they reduce the quantum efficiency of the sensor. Fortunately, half of the pixels are well matched to common green-emitting phosphors such as Gd₂O₂S:Tb.

Most of the new DSLRs use CMOS (complementary metal oxide semiconductor) sensors rather than CCDs (charge-coupled devices), which means that they have circuitry for charge integration, preamplification, noise control and readout switching at each individual pixel. This circuitry greatly improves the camera’s noise performance (see Sec. 2.4), but it reduces the silicon area that is available for the photosensors, and that in turn would further reduce the quantum efficiency were it not for two clever optical tricks employed by most of the major DSLR manufacturers. The first is to use an array of microlenses to concentrate light on the active sensor area. For light arriving at the sensor at normal incidence, each microlens focuses the light into the center of its photodetector element, but for non-normal incidence the light could be diverted to the insensitive areas between photodetectors.

This latter problem is avoided with so-called “digital” lenses, which just means that they are intended to be used with digital cameras. The important feature of digital lenses is that they are telecentric in image space, so the chief ray is always perpendicular to the sensor plane and hence parallel to the optical axes of the microlenses. The result is that nearly all of the light transmitted by the lens and color filters arrives at the active area of the CMOS sensor.

Canon, Nikon and other manufacturers supply fixed-focus (non-zoom) F/1.4 digital lenses for full-field DSLRs. Older lenses designed with use with 35 mm film cameras such as the Nikkor 50 mm, F/1.2, can also be used, but sensitivity at high field angle will be sacrificed because the lenses are not telecentric. Specialty lenses as fast as F/0.7 are available on the surplus market, but they do not usually cover the full FX format.

2.2. Spatial resolution

The full-field DSLR sensors all have nominally either 12 or 24 megapixels (MP). The 12 MP cameras (e.g., Canon 5D or Nikon D700) have approximately a 2800 × 4300 array of 8.5 μm × 8.5 μm pixels, and the 24 MP cameras (e.g., Canon 5D Mark II or Nikon D3X) have approximately a 4000 × 6000 array of 6 μm × 6 μm pixels. If we consider 12:1 demagnification as for chest radiography, the 12 MP cameras provide effectively 100 μm × 100 μm pixels at the x-ray screen, and the 24 MP cameras provide 72 μm × 72 μm pixels. Larger effective pixels can readily be achieved by binning the sensor pixels during readout.

Fixed-focus lenses designed for use with full-field DSLRs and used at full aperture typically have about 30 lp/mm resolution at 50% MTF, which corresponds to a focal-plane resolution of about 15 μm FWHM. At a demagnification of 12:1, therefore, the lens contribution to the resolution at the x-ray screen is about 2.5 lp/mm at 50% MTF or 180 μm FWHM.

The other significant contributor to spatial blur is the screen itself. Lanex screens ($\text{Gd}_2\text{O}_2\text{S:Tb}$) yield resolutions in the range 1 – 3 lp/mm at 50% MTF depending on the speed of the screen. Columnar CsI screens, now available in chest size, can be as good as 5 lp/mm at 50% MTF and a thickness of 150 μm [3]. The demagnification does not affect the screen contribution to the resolution.

2.3. Noise

A major concern with using DSLRs for DR is collecting sufficient light from the x-ray screen [4]. At 10:1 demagnification, a standard F/1.4 camera lens will collect about 0.1% of the light emitted by a Lambertian source. Measured conversion efficiencies (from x-ray energy to optical energy) of $\text{Gd}_2\text{O}_2\text{S}$ or $\text{La}_2\text{O}_2\text{S}$ screens is in the range 18 - 20% [5], which means that a single 50 keV x-ray photon will yield approximately 4,000 optical photons, each of energy around 2.5 eV (green). If we collect 0.1% of them, then only 4 photons will reach the camera sensor, and if the sensor quantum efficiency is around 25% (see Sec. 2.1), we get around 1 photoelectron per x-ray photon. These numbers improve somewhat if we use an F/1.2 lens or if we consider a smaller demagnification, and they could be improved further by removing the color filter or using one of the new brighter phosphors such as columnar CsI or LaBr_3 .

In addition to the x-ray photon noise, the noise generated in the DSLR, referred to generically as read noise, is a major issue. The potential contributors to read noise are dark current; kTC noise, which arises from resetting the gated integrators in either CMOS or CCD sensors; thermal noise in the electronics, and 1/f or flicker noise. Of these components, we can readily dismiss dark-current noise, which is negligible compared to the other noise sources for the short exposures used in x-ray imaging. Similarly, pure thermal (Johnson) noise is negligible compared to kTC and 1/f noise in most practical sensors. With respect to these two remaining noise sources, modern CMOS sensors have a huge advantage over CCD sensors, even over expensive scientific-grade cameras, basically because they place a lot of electronic circuitry at the individual pixels rather than at the end of a charge-transfer chain as with a CCD [6].

To understand this point, consider first kTC noise, which is endemic in both CMOS and CCD sensors. In both, the charge produced by the light is converted to a voltage by storing it on a capacitor, which should be reset to zero after each conversion. Basic thermodynamics, however, shows that the residual voltage on the capacitor cannot be truly zero but instead fluctuates with a variance of kT/C (k = Boltzmann's constant, T = absolute temperature, C = capacitance). One way of suppressing kTC noise (which really should be called kT/C noise) is a process called correlated double sampling (CDS) in which the voltage on the capacitor is measured after each reset and then again after the charge is stored and before the next reset; the difference between the readings is proportional to the photoinduced charge with little residual error from the thermodynamic effects. Alternatively, a process called active reset can be used in which feedback control drives the residual voltage on the capacitor close to zero.

In a modern CMOS sensor, there is an integrating capacitor and a CDS or active-reset circuit at each pixel. The capacitor is reset and the sensor is exposed to light for a frame period (100 - 200 msec for a sensor that operates at 5 - 10 frames per second, as many DSLRs do), and then the capacitor is reset again. The CDS or active-reset circuit must therefore operate only once per frame, but the circuits at all pixels can operate in parallel, so the overall processing rate is millions of times higher. In a CCD, by contrast, the signal remains in the form of charge until it is shifted out to a capacitor. There is just one reset and CDS or active-reset circuit, and it must operate serially at the pixel rate rather than the frame rate.

There is a similar advantage to CMOS detectors with respect to thermal and 1/f noise, both of which have a variance that is proportional to bandwidth. The lower circuit bandwidth associated with parallel processing at the pixel level automatically results in lower noise, and 1/f noise is further suppressed by CDS at the pixel level [6]. As a result, low-noise, scientific-grade CCDs are often read out at only 50,000 pixels per second, while prosumer DSLRs can go over a thousand times faster.

An excellent source for quantitative comparisons of CCD and CMOS cameras and sensors is the Clarkvision website [7]. Tables and graphs given there show that prosumer DSLRs typically have an RMS read noise equivalent to about 3-5 electrons, but scientific-grade CCD cameras and sensors can be up to ten times worse, in spite of their much higher cost and much lower bandwidth.

3. IMAGE QUALITY AND DQE

A simple way to understand the effect of read noise on objective (task-based) image quality is to assume that all of the light emitted from a single x-ray interaction and collected by the lens ends up on a single pixel in the camera sensor. With the numbers given in Sec. 2.2, this might be a valid assumption if we use 2×2 or 3×3 pixel binning.

With this assumption, the performance of an ideal linear (Hotelling) observer [8] for the task of detecting a known signal on a known background can readily be derived. The details will be published separately, but the Hotelling detectability is given by

$$SNR_{Hot}^2 = \sum_{m=1}^M \frac{\bar{k}^2 (\Delta \bar{N}_m)^2}{\sigma_{read}^2 + \bar{N}_m (\bar{k} + \bar{k}^2)} \quad (1)$$

where the sensor contains M pixels, each of which is denoted by an index m ; σ_{read}^2 is the variance of the read noise (expressed in electron units and assumed to be the same for all pixels); \bar{N}_m is the mean number of x-ray interactions imaged to pixel m when there is no signal present; $\Delta \bar{N}_m$ is a small change in that number when a signal is present, and \bar{k} is the mean number of photoelectrons produced by each x-ray interaction (again assumed to be independent of m).

Following Gagne et al. [9], we can define a task-specific DQE (detective quantum efficiency) by dividing the Hotelling detectability for the actual detector by the detectability on the same task for an ideal detector that has no read noise and $\bar{k} \gg 1$. For the task of detecting a uniform disk object on a flat background, we find

$$DQE = \frac{\bar{k}^2 \bar{N}}{\sigma_{read}^2 + \bar{N} (\bar{k} + \bar{k}^2)} \quad (2)$$

where \bar{N} is the common value of \bar{N}_m for all pixels in the disk region. If the disk region is large compared to the optical blur, for example for detection of a 1 mm lesion, this same expression is obtained even without assuming that all of the light from one x-ray photon is imaged to a single camera pixel.

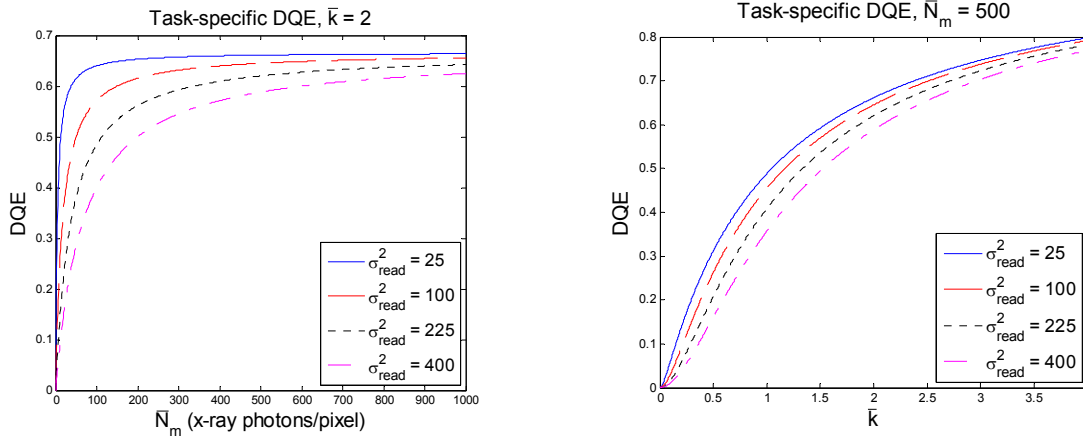


Fig. 1. DQE for detection of a uniform disk lesion on a flat background. Left: DQE vs. x-ray fluence (absorbed photons per 100 μm pixel) for fixed optical efficiency (2 photoelectrons per x-ray photon) and difference camera read-noise variances. Right: DQE vs. optical efficiency for different x-ray fluences and noise levels. Typical \bar{N}_m in DR is 500 photons per pixel, and typical σ_{read}^2 in a modern DSLR is about 25 (5 electrons RMS).

The dependence of DQE on read noise, optical efficiency and x-ray fluence is shown in Fig. 1. Several limits are of interest. If there is no read noise but the lens is very inefficient so that $\bar{k} \ll 1$ the equation above predicts that the DQE of the detector (not including the x-ray screen) is simply \bar{k} . If there is no read noise but the lens is sufficiently efficient that $\bar{k} \gg 1$, then we get DQE = 1. The case of interest in this paper, however, is when $\bar{k} \sim 1$ and the read noise is not zero. In that case, we can still get nearly quantum-limited performance, provided the x-ray fluence is high enough; if $\bar{N}_m(\bar{k} + \bar{k}^2) \gg \sigma_{read}^2$, then the read-noise term in the denominator can be neglected and the DQE is $\bar{k}^2/(\bar{k} + \bar{k}^2)$. In order to do high-quality DR with a DSLR, therefore, it is very important to choose a camera with low read noise.

4. PROTOTYPE SYSTEM

Based on cost and the design considerations above, we chose a Nikon D700 camera with an AF-S Nikkor 50mm f/1.4G lens for the prototype. We elected not to use a folding mirror, so the x rays transmitted by the screen impinged on the camera. By measuring the x-ray transmittance of the lens, however, we found that x-ray flux on the camera sensor was very small. No radiation damage was expected, and with several thousand x-ray exposures to date, none has been observed.

The system is constructed on an extruded aluminum frame that folds down into a small suitcase as shown in the left photo of Fig. 2. The vertical assembly on the right in that photo is an opaque bakelite sheet with a standard Lanex screen mounted on the side facing the camera. The screens are interchangeable, and both Lanex Regular and Lanex Fast have been used. There is a light-tight felt cloth shroud, shown in the right photo of Fig. 1, and only a thin camera cable needs to emerge from the shroud during operation.

For transport, the suitcase contains the aluminum frame and x-ray screens, the shroud, a laptop computer, a solar panel for charging the computer and camera, a dosimeter and miscellaneous tools. Exclusive of the camera, which was carried separately, it weighs about 45 pounds. The total cost of the system, including the camera, laptop and lens, was less than \$5,000.



Fig. 2. Left: Prototype DR system showing x-ray screen on the right and Nikon D700 DSLR on the left. The frame folds down into the suitcase for transport. Right: Same system but with light-tight shroud in place. System is shown as set up in the Manang District Hospital, Chame, Nepal, with the breast phantom in position for imaging.

5. RESULTS

The prototype system was taken to Nepal in spring, 2009, and tested in two clinics in the Kathmandu valley and in two district hospitals along the Annapurna Circuit Trail. All locations had existing x-ray tubes, so no x-ray source was transported.

A standard breast phantom was imaged with varying kVp and mAs and camera ISO settings at all four locations in Nepal and also in the Radiology Department of the University of Arizona. Comparison film-screen images were obtained at the Nepali locations, and Computed Radiography (CR) images were obtained in Arizona. Radiation exposure incident on the phantom was measured in all cases.

A sample comparison is shown in Fig. 3. The film image on the right was acquired in Nepal but brought back to Arizona and digitized by photographing it with the Nikon D700 camera, trying to match the contrast presentation with that of the DSLR image on the left as closely as possible. All features of interest are visible in both images, but uneven development and several white blotches, probably from foreign matter on the screen, are evident on the film-screen image.

A second comparison, conducted entirely in Arizona, is illustrated in Fig. 4. In this case a human skeleton embedded in plastic was the phantom, and the comparison was between the DSLR system and a Fuji CR system. The exposure conditions, noted in the caption, are not identical in this case, but we again made an effort to match the display contrasts. There is no evident difference in feature visibility, but of course this is not a definitive statement. A more detailed ROC-based comparison is planned, and the results will be reported separately.

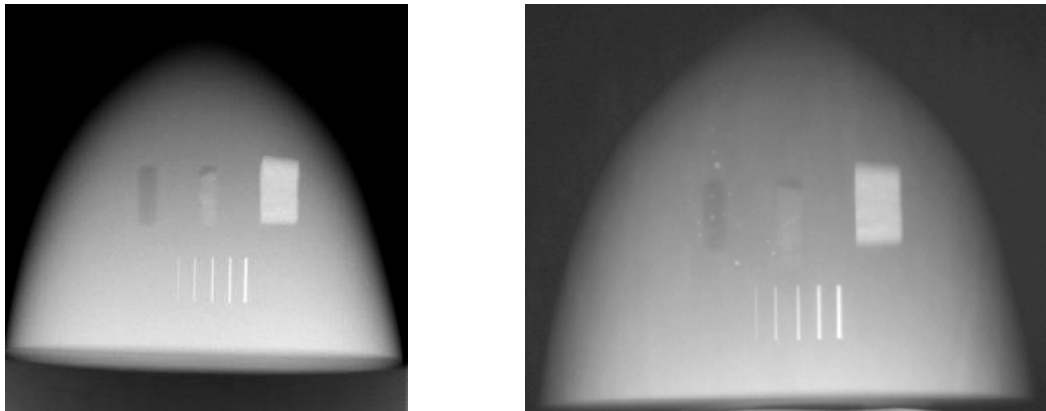


Fig. 3. Images of the breast phantom taken with the same exposure in a Himalayan clinic in Nepal. Left: Image taken with the DSLR system. Right: Image taken with local film-screen technique.

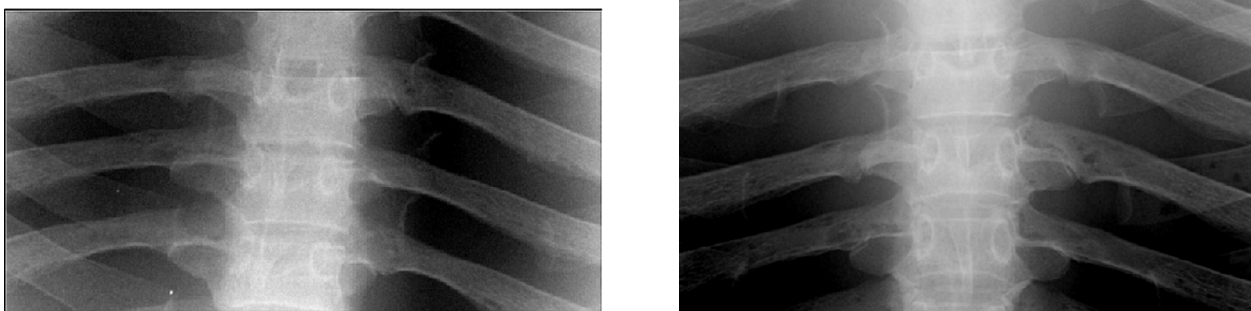


Fig. 4. Magnified portions of chest-phantom images taken at the University of Arizona with two different DR systems. Left: DSLR system, 80 kVp, 25mAs, ISO 4000. Right: Fuji XG5000 Computed Radiography system, 109 kVp, 10 mAs.

6. SUMMARY AND CONCLUSIONS

When used with conventional x-ray screens, modern prosumer DSLRs are attractive detectors for DR. Compared to other consumer digital cameras, they have much lower read noise and substantially larger sensors, reducing the demagnification factor needed to cover a given FOV and hence increasing the light-collection efficiency. The use of microlenses to direct the light to the photosensitive region of each pixel along with telecentric “digital lenses” results in a sensor fill factor of, effectively, 100%. For large fields of view (e.g., chest radiography), the optical collection efficiency is approximately 1 photoelectron per x-ray interaction, but this number can be improved either by using smaller fields or by removing the color filter on the camera. Because the DSLR read noise is so low, the DQE (not including the screen absorption) for a disk-detection task can exceed 50%.

Compared to scientific-grade CCD cameras, the DSLRs have large advantages in cost, read noise and readout speed. They cannot compete with CCDs in terms of quantum efficiency or dark current, but neither of these characteristics is critical for DR.

Compared to current CsI or amorphous selenium flat-panel detectors, the main advantage of the DSLR approach is cost and readout speed. The resolution and noise performance of the DSLR system may be comparable to those of flat-panel detectors, but more studies are needed to confirm this conjecture.

Compared to film-screen systems in rural clinics, a major advantage of the DSLR approach is the digital character of the data. A DSLR provides an instant digital image for display manipulation and telemedicine, and it eliminates concerns about control of the developing process. Moreover, the large dynamic range of the cameras should lead to fewer incorrect exposures than with film. The DSLRs may also offer advantages over film-screen in terms of resolution, noise and the dose required for equal objective image quality, but many more studies are needed.

Finally, we note that the DSLR approach has the potential to bring fluoroscopy into rural settings; some DSLRs can take continuous data at 30 fps.

ACKNOWLEDGEMENTS

This work was supported in part by the National Institutes of Health grants T32 EB000809 and P41 EB002035 and by the State of Arizona Technology Research Infrastructure Fund.

REFERENCES

- [1] Wootton, R., Patil, N. G., Scott, R. E. and Ho, K., Editors, [Telehealth in the Developing World], Royal Society of Medicine Press/IDRC (2009).
- [2] Graham, K. E., Zimmerman, M., Vassallo, D. J. et al., “Telemedicine--the way ahead for medicine in the developing world,” *Tropical Doctor*, 2003, 33, 36-38 (2003).
- [3] Nagarkar, V., Gupta, T., Miller, S., Klugerman, Y., and Squillante, M., “Structured CsI(Tl) scintillators for X-ray imaging applications,” *Conference Record, IEEE Nuclear Science Symposium*, Albuquerque, NM, (1997).
- [4] Hejazi, S., and Trauernicht, D. P., “System considerations in CCD-based x-ray imaging for digital chest radiography and digital mammography,” *Med. Phys.* 24 (2), 287- 297 (1997).
- [5] Kandarakis, L., and Cavouras, D., “Experimental and theoretical assessment of the performance of $Gd_2O_2S:Tb$ and $La_2O_2S:Tb$ phosphors and $Gd_2O_2S:Tb - La_2O_2S:Tb$ mixtures for x-ray imaging,” *Eur. J. Rad.* 11, 1083-1091 (2001).
- [6] Magnan, P., “Detection of visible photons in CCD and CMOS: A comparative view ,” *Nuclear Instruments and Methods in Physics Research A* 504, 199–212 (2003).
- [7] <http://www.clarkvision.com/imagedetail/digital.sensor.performance.summary/>
- [8] Barrett, H. H., and Myers, K. J. [Foundations of Image Science], Wiley, New York (2004).
- [9] Gagne, R. M., Boswell, J. S. and Myers, K. J., “Signal detectability in digital radiography: Spatial domain figures of merit,” *Med. Phys.* 30(8), 2180-2193 (2003).